Journal of Petroleum Research and Studies

Open Access
No. 38, March 2023, pp. 74-96

P- ISSN: 2220-5381
E- ISSN: 2710-1096

DOI: http://doi.org/10.52716/jprs.v13i1.673

Thermal Analysis of Absorption Air Conditioning Cycle Using Glycerin in Hot and Cold Storage Tanks

Murad N. Mardan[1*], Yaareb Elias Ahmed[2], Maher K. daham[3], Safad A. Hussein[4]

[1,4]North Oil Company / Oil Exploration Company / Ministry of Oil / Kirkuk, Iraq

[2]Kirkuk Gas Power Plant / State Company of Electricity Production/ Ministry of Electricity / Kirkuk, Iraq

[3]Technical Institute of Hawija, Northern Technical University, Kirkuk, Iraq

[1*]Corresponding author: engmuradnehad1985@gmail.com

[2]yaarub_hwj@ntu.edu.iq, [3]Maher.khalil89@gmail.com, [4]safadali527@gmail.com

Received 19/6/2022, Accepted in revised form 4/8/2022, Published 15/3/2023

Abstract

Increasing demand for cooling operations in the oil and other sectors, this has led to an increase in electrical energy consumption. The most sustainable solution is to use absorption cooling technology by utilizing solar heat as driving energy instead of electricity. The primary advantage of absorptive cooling is lower electricity costs. In this study, the effect of changing the thermal storage capacities of hot and cold storage tanks and the solar collector area on the performance of the absorption air conditioning cycle was investigated. The optimum operating conditions, the maximum number of processing hours, and the optimum performance coefficient of the absorption conditioning cycle system were selected. The water-lithium bromide solution was used as a fluid in the sorption cycle, and glycerin was used in the hot and cold tank cycle and in the solar collector because it can with stands both high and low temperatures.

The simulation process was carried out using (Fortran 90) program with the help of (Port log) program, (Carrier HAP420) program and (Curve Expert) program. The absorption conditioning cycle was simulated during the day to choose the best capacity for hot and cold storage tanks, as well as to choose the solar collector with the best performance factor. Changing the area of the solar collector (from 9.6 m^2 to 16.7 m^2), and the volume of the hot tank (from 0.55 m3 to 1.4 m3) have been done to provide the maximum temperature that the hot tank can reach with varying expected cooling load per hour, as well as the size of the tank cold (from 0.9 m3 to 1.6 m3) which gets additional cooling capacity, since the effect of these variables was tested separately.

According to the research results, the best and most suitable volume for the hot tank is (0.55 m3), and for the cold tank is (1.5 m3), and the best and appropriate area for a solar concentric

Open Access
No. 38, March 2023, pp. 74-96

P- ISSN: 2220-5381
E- ISSN: 2710-1096

collector is (11.7 m^2), which can provide longer running hours. Finally, the higher the generator's temperature, the higher the system's coefficient of performance (COP). The lowest COP value (0.68) is used to guarantee that the system runs for longer periods of time.

Keywords: Absorption Cycle, Hot and cold storage tanks, Lithium bromide-water solution, Glycerin, Solar collector.

تحليل حراري لدورة تكييف الهواء الامتصاصية بأستخدام الكَلسرين في خزانات التخزين الحارة والباردة

الخلاصة:

مع تزايد الطلب على عمليات التبريد في النفط والقطاعات الأخرى ، أدى ذلك إلى زيادة استهلاك الطاقة الكهربائية. الحل الأكثر استدامة هو استخدام تقنية التبريد بالامتصاص من خلال استخدام الحرارة الشمسية كطاقة دافعة بدلاً من الكهرباء. الميزة الأساسية للتبريد الامتصاصي هي انخفاض تكاليف الكهرباء. في هذه الدراسة، تم التحري عن دراسة تأثير تغيير كل من سعات التخزين الحرارية للخزانات الساخنة والباردة ومنطقة المجمع الشمسي على أداء دورة تكييف الهواء الامتصاصية. حيث تم اختيار أفضل ظروف التشغيل، والحد الأقصى لعدد ساعات المعالجة، والوصول إلى أفضل معامل الأداء لنظام دورة تكييف الامتصاص. تم أستخدام محلول بروميد الليثيوم-الماء كمائع في الدورة الأمتصاصية، وأستخدام مادة الكَليسرين في دورة الخزانات الساخنة والباردة وفي المجمع الشمسي لأنها تتحمل درجات الحرارة العالية والمنخفضة.

تمت عملية المحاكاة باستخدام برنامج (Fortran 90) بمساعدة برنامج البورت لوك (Port log)، برنامج (Carrier HAP420) وبرنامج (Curve Expert). حيث تم محاكاة دورة التبريد الامتصاصية خلال اليوم لأختيار أفضل سعة لخزانات التخزين الساخنة والباردة، كذلك لأختيار المجمع الشمسي بأفضل معامل أداء. تم تغيير مساحة المجمع الشمسي (من 9.6 م2 إلى 16.7 م2)، وحجم الخزان الساخن (من 0.55 م3 إلى 1.4 م3) لتوفير أقصى درجة حرارة يمكن أن يصل إليها الخزان الساخن مع اختلاف حمل التبريد المتوقع لكل ساعة، وكذلك حجم الخزان البارد (من 0.9 م3 إلى 1.6 م3) الذي يحصل على سعة تبريد إضافية ، حيث تم اختبار تأثير هذه المتغيرات بشكل منفصل. وبحسب نتائج البحث فإن أفضل وأنسب حجم للخزان الساخن هو (0.55 م 3) ، وللخزان البارد (1.5 م 3) ، وأفضل مساحة مناسبة للمجمع الشمسي المركزى (11.7 م 2) ، والتي يمكن أن توفر ساعات تشغيل أطول. أخيرًا ، كلما ارتفعت درجة حرارة المولد ، زاد معامل أداء النظام (COP). يتم استخدام أدنى قيمة COP (0.68) لضمان تشغيل النظام لفترات زمنية أطول.

1. Introduction

Population expansion, modern transportation, industry, and a variety of other factors all contribute to rising demand for conventional energy around the world. The creation of hazardous gases, which increases the thermal retentions, has an impact on the environment. Solar energy is the most important renewable energy source, with applications in a variety of fields. Energy acquired from environmentally friendly sources reduces thermal retentions and pollutants [1]. Many nations throughout the world suffer an issue of increasing electric power consumption, particularly during the midday in the summer, due to the usage of high-energy traditional air conditioners. Solar energy has been presented as a strategy for preventing this problem by impacting the ozone layer [2, 3]. The researchers recommend that solar energy be used to

Open Access
No. 38, March 2023, pp. 74-96

P- ISSN: 2220-5381
E- ISSN: 2710-1096

generate the thermal energy of absorption cooling system. This is a versatile method of converting solar energy into electricity that employs a variety of solar collectors, such as flat and parabolic concentric solar collectors. The goal is to generate the most thermal energy feasible. These collectors were utilized in the absorption cooling systems directly [4]. The system's primary and most important component is the generator. The solar collectors provide it with thermal energy. For lengthy periods of time, it has been observed that using solar collectors directly in an absorption cooling systems is suitable to the air conditioning conditions [5]. That because the solar collectors process thermal energy based on the intensity of solar radiation through the day. This is, however, improper at night, as well as on dusty or cloudy periods [6]. Adding a thermal storage-tank to the system for solving this problem by prolonging the energy storage during the day, and then continuing to provide the required temperature of thermal-energy collected when the solar intensity weakens. [7]

Authors performed research and developed concepts for using solar energy to generate heat energy in conjunction with an absorbance cooling systems to conditioning the region. In study [8], a parabolic-solar collector with a surface area of 7.5 m^2 was tested for a hot tank capacity of 0.23 m3 utilizing therminol 55 fluid and a mass flow rate of 0.1 kg/s via the solar detector. On a sunny day, the highest fluid temperature is 116°C, while on another sunny day, the maximum fluid temperature is 212°C during the midday (12 p.m.) time. The gained heat is determined to be below the thermal losses after (2 p.m.). As a result, after 2 p.m., the cycle would never be used. The modeling [9] is used to determine the best size of a hot storage tank for a solar collector absorption cooling system. The solar collector is 50 m2 in area, with a cooling capability of 35 kW and a capacity of 2 m^3 for the hot tank. The solar collector's theoretical area was less than 65 m^2, with a capacity of (35 kW) absorption-cooling system and a tank-capacity ranging from (0.1 to 0.5 m^3). The best hot-tank capacity was 0.1 m3, according to the results.

The utilization of various solar collectors, such as flat or focused solar collectors, to obtain the best available thermal energy is investigated in a solar thermal air-conditioning systems working with lithium-bromide solution and water [10]. [11] investigates the influence of cold and hot storage-tanks in order to determine the feasibility of increasing the number of system working hours. A cold tank is used to hold excess coolant in order to cover the load for the specified time period. In a university building's, an absorption cooling system is evaluated for 4-classrooms using experimental and analytical methods [12]. The solar collector has a surface area of 90 m^2,

Open Access
No. 38, March 2023, pp. 74-96

P- ISSN: 2220-5381
E- ISSN: 2710-1096

and the absorbing cooling system has a capacity of 30 kW and 70 kW for the cooling tower, 1.5 m^3 and 1 m3 for the hot and the cold tanks respectively. The writers employ 13 coil and fan units that are distributed around the classrooms. The operation system is set at 80°C. According to the findings, the average error for calculating the used energy produced over the duration of a day in May is 0.5%. For the generated power in the evaporator on the same day, the average error is 2.7%. [13] investigates the impact of thermal storage on a medium-sized building's solar-absorption cooling system. The process is designed to deliver 50% of the total cooling load for the building. The solar collator has a surface area of 200 m^2, and the absorption system's cooling energy is 120 kW. According to the research, increasing the cold tank volume from 2 to 22 m^3 causes the solar fracture to increase from 51 to 57%. Furthermore, the solar cooling system is highly dependent on the size of the solar collector, the capacity of the chiller, and the capacity of the cold and cold storage tanks. Absorption-cooling system with solar energy as a thermal supply is studied experimentally and theoretically in [14]. Lithium bromide–water solution is used as the absorbent material. [15] conducts an experimental investigation to evaluate the efficacy of an absorption-cooling system for a 10ton Li-Br/H_2O system. The absorbent material is Lithium bromide–water solution, and the heat source is solar energy. In [16], the optimal control system for an absorption cooling system using solar energy as a thermal source and lithium bromide solution-water as the absorbent material was examined.

In [17], a theoretical analysis of a TRNSYS model was carried out to analyze the performance of an absorption cooling system that employs solar energy as a thermal source and a lithium bromide solution as the absorbent material. At the University of New Mexico, the system is utilized to cool the bottom floor of the mechanical engineering building. [18] does a theoretical analysis of HVAC systems in order to evaluate the efficacy of absorption cooling systems. The absorbent substance is lithium bromide solution, and the heat source is solar energy. The system is in operation at the University of New Mexico to cool the engineering building. [19] describes a simulation of an absorption cooling system that uses solar energy as a thermal source and a lithium bromide (LiBr/H_2O) solution-water as the absorbent medium. The technology is being utilized to cool an 82-square-meter office space at the University of Cardiff. [20] conducts a theoretical analysis to evaluate the performance of an absorption cooling system. They used this device to show the impact of thermal storage. [21] presents a practical and theoretical investigation to evaluate the effectiveness of an absorption cooling system in a tropical region.

Open Access
No. 38, March 2023, pp. 74-96

P- ISSN: 2220-5381
E- ISSN: 2710-1096

[22] conducts a theoretical analysis to evaluate the efficacy of an absorption cooling system using green freeze technology. Solar energy is employed as a heat source, and the absorbent substance is lithium bromide solution. [23] conducts a theoretical investigation of heat transport through a solar space filled with a porous material. [24] investigates a hybrid CFD-ANN technique for airflow and heat transport through an array of in-line flat tubes. [25] performs modeling and simulation of a desiccant evaporative cooling system.

In the research [26], a digital model was implemented to verify the performance of the building's cooling system. The system is powered by a solar powered absorption cooling system using a concentric parabolic solar collector combined with thermal storage tanks. The building area is 40 m2 and its hourly load is calculated, the volume of thermal storage tanks (cold and hot) ranges from (0.2 to 1.25 m^3) and this takes place in the area range (10 to 30 m^2) of a concentric parabolic sump collector. The results showed that the typical volume of a hot storage tank is 0.23 m^3 and the volume of a cold storage tank is 0.57 m3 at the lowest solar collecting area of 16.6 m^2 to condition the building during most of the daylight hours from 11 am to 6 pm. The maximum value of COP is 0.65 based on the optimal parameters. The study [27] aims to examine the electrical and thermodynamic performance of a tri-hybrid vapor absorption-assisted air conditioning system versus a conventional system with the help of Energy-Plus simulation software for a small office building. The performance of the absorption system is evaluated at different temperatures of the generator (70°C - 80°C) and the solar collecting area (400 m^2 to 500 m^2). The results showed that by using the absorption-based systems, a maximum saving of 34.1% of electrical energy can be ensured in a collection area of 500 square meters with a generator temperature of 70°C. Under the condition of the generator temperature is 70°C and the collector area is 500 m^2, the absorption system can be made to be based on fully renewable energy. In the work [28], design and thermo-economic analyzes are presented to compare two different types of collectors (equivalent trough and evacuated tube) by lithium-bromide water absorption systems. In general, the main component of the system is absorption refrigeration chiller, solar thermal energy conversion system, condenser and absorption refrigerant and cold circuit and useful refrigeration power plants produced. A case study was presented for a sports arena with a total cooling load of 700-800 kW. The results reveal that a parabolic trough complex with H2O-LiBr (PTC/H2O-LiBr) gives fewer design aspects and minimal hourly costs.

Open Access
No. 38, March 2023, pp. 74-96

P- ISSN: 2220-5381
E- ISSN: 2710-1096

The goal of the study is to determine the best thermal storage for the absorption cycle by measuring the temperature of the hot and cold storage tanks in which glycerin is utilized. Also the cold tank's cooling capability used for cooling is evaluated. Finally, the appropriate capacity for the hot and the cold tanks are figured.

2. The System Working Principle

A parabolic concentric collector, lithium-bromide-water solution absorption chiller, and a cold-storage tank form the components of a solar absorption cooling system shown in Figure (1-a). Thermal solar energy is collected using the parabolic concentric collector. The hot storage tank is then used to store the solar thermal energy [23, 24]. The glycerin in the hot storage tank feeds the absorption chiller. The heated glycerin is then sent to the generator, which is used to generate water-vapor from a lithium bromide and water solution. The water-vapor is cooled in the condenser using high pressure cooling. The vapor is then sent to the evaporator through an expansion valve. The water vapor is then evaporated by the low pressure. The operational-fluid in the evaporator cools the conditioned area to meet the building's cooling load, and the surplus cools the glycerin in the cold-storage tank. The saturated vapor is absorbed by a high-percentage of lithium bromide solution and water in the absorber container. The saturated vapor is then sent through the heat exchanger to the generator [25]. Figure (1-b) shows the single effect absorption cycle of lithium bromide – water.

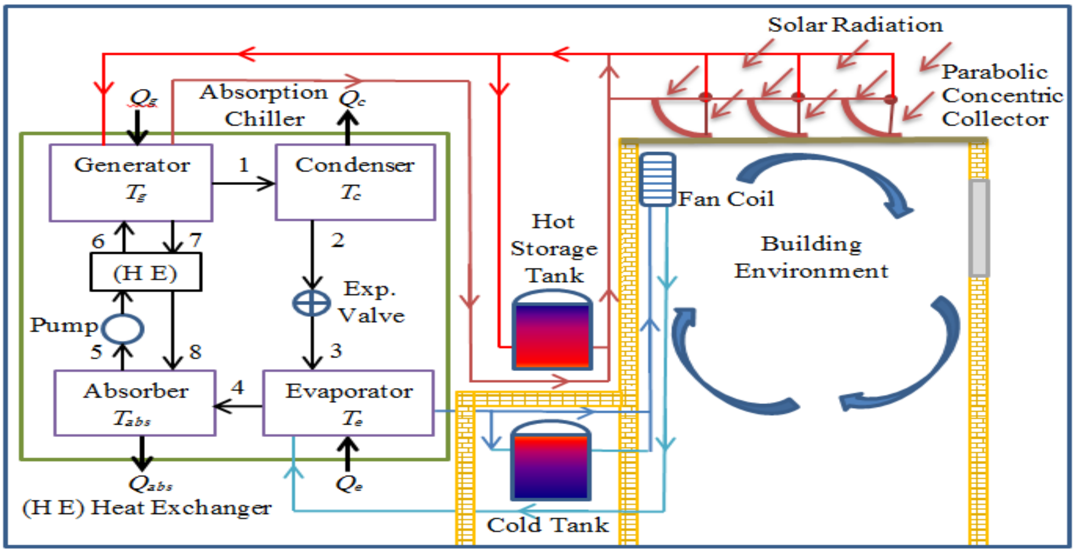

(a)

Open Access
No. 38, March 2023, pp. 74-96

P- ISSN: 2220-5381
E- ISSN: 2710-1096

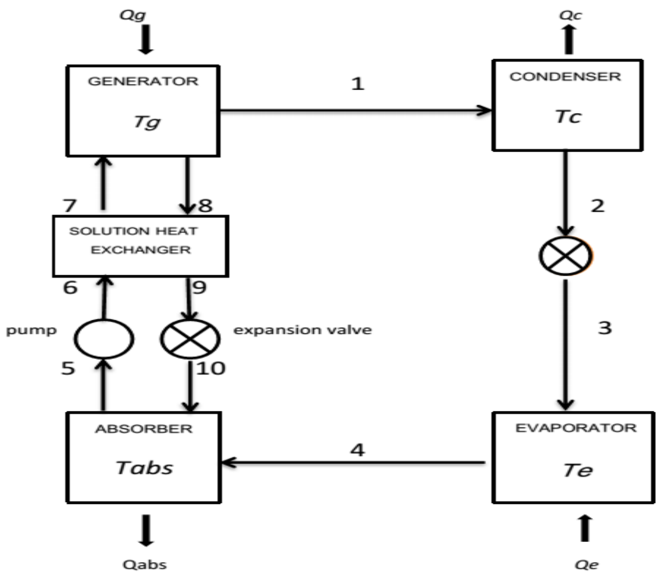

(b)

Fig. (1): (a) The overall schematic diagram of the cooling system, (b) Single effect absorption cycle of lithium bromide – water.

To cover the air conditioning load in the conditioned zone, chilled glycerin provides cooling energy. The unused coolant is stored in the cold storage tank. In the case that solar energy is insufficient or unavailable, additional coolant is given to the conditioned space [29]. The results obtained in this study are similar to those reported by the authors in [30]. Figure (2-a) illustrates the energy supply to the cold tank, while Figure (2-b) shows the energy discharge to chill the conditioned space.

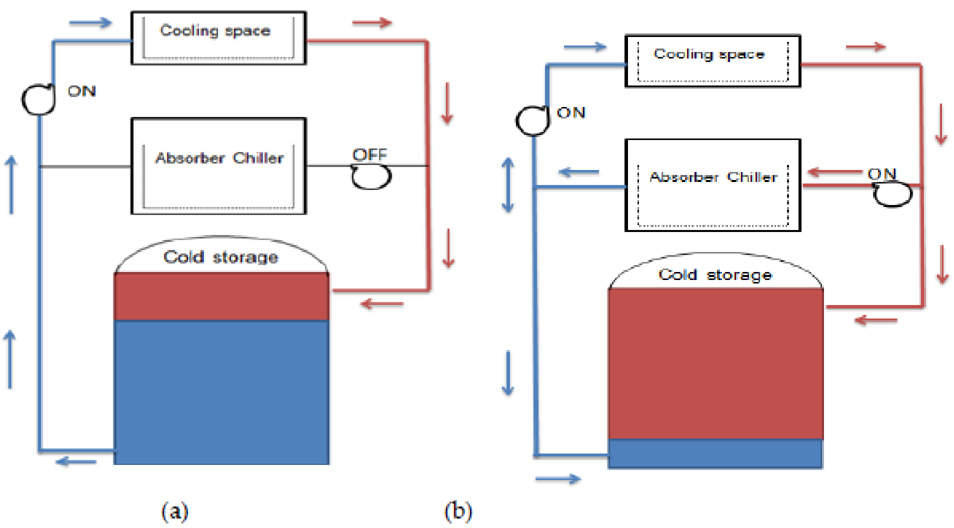

Fig. (2): (a) Charging a cold tank (b) Energy exchange in a cold tank.

Open Access
No. 38, March 2023, pp. 74-96

P- ISSN: 2220-5381
E- ISSN: 2710-1096

The simulation of the multiple elements, such as the solar collector, absorption cooling system, cold storage tank, and hot storage tank, relies on a number of assumptions like fluid characteristics are constant, the flow through the absorber-tube is in a steady-state, the pressure is constant in the absorber internal tube, and heat transferred by conduction along the absorber-tube is ignored in solar thermal. When heat is transferred by convection, the key assumptions of the hot storage tank are that all sides are insulated, energy loss in tubes are ignored, and the tank temperature is uniform and less than the evaporation-temperature of the used liquid. The major assumptions of the absorption cooling system are that the generator and condenser pressures are equal, the absorber and evaporator pressures are the same, the generator and evaporator exit fluids are saturated, and the pressure loss in the pipes is ignored. Finally, the cold storage tank's basic assumptions are that the initial temperature of the tank is equals to the ambient temperature, which would be equals to or less than 28ºC, the losses by thermal conduction in the pipe are neglected, and the tank temperature is higher than the glycerin's freezing temperature.

The simulation process was carried out by programming mathematical equations using the program (Fortran 90) with the help of several sub-programs that are used to enter several variables in order for the simulation process to take place. Whereas, the process of measuring and recording the required variables for climate data in the city of Kirkuk was done electronically by the Port log program. And then pull this data by linking the device with the calculator and downloading the data according to the required time intervals. While the cooling load can be obtained for every hour of the day using the Carrier HAP420 program, and through it becomes possible to calculate and determine the thermal loads and this leads to the possibility of determining and choosing the capacity of the absorption cooling system required for air conditioning. On the other hand, (Curve Expert) program was used to find the equations needed to change the physical properties of glycerin with temperature.

3. Mathematical Modeling

3.1. Thermal Solar Collector Mathematical Modeling

The efficiency of solar thermal concentrated collector can be determined as follows [30]:

$$\eta = \frac{Q_{usf}}{I_b\, A_{ape}} \qquad (1)$$

Open Access
No. 38, March 2023, pp. 74-96

P- ISSN: 2220-5381
E- ISSN: 2710-1096

The useful heat Q_{usf} can be calculated actually as follows:

$$Q_{usf} = A_{ape} F_R \left[H_{ab} - \frac{A_{rto}}{A_{ape}} U_L \left(T_{g,i} - T_{amb} \right) \right] \tag{2}$$

$$A_{ape} = w \times L \tag{3}$$

$$A_{rto} = \pi \; D_{rt,o} \, L_{rt} \tag{4}$$

Absorbed solar energy can be defined as:

$$H_{ab} = I_b \tau \alpha \rho \gamma \times \cos\theta \tag{5}$$

The overall coefficient of the heat loss U_L (W/m^2.^{o}C) in the glass-tube is calculated as:

$$U_{\text{L}} = h_{win} + h_{ra,rt-sky} \tag{6}$$

The wind speed heat transfer coefficient is expressed as [31]:

$$h_{win} = 4 D_{rt,o}^{-0.42} \times V^{0.5} \tag{7}$$

Between the absorber tube and its surroundings, the heat transfer coefficient by radiation (W/m^2.^{o}C) is stated as [30]:

$$h_{ra,rt-sky} = \varepsilon_{rt} \, \sigma \left[T_{rt} + T_{sky} \right] \left[T_{rt}^2 + T_{sky}^2 \right] \tag{8}$$

The temperature of sky (^{o}C) can be expressed by:

$$T_{sky} = 0.055 \, T_{amb}^{1.5} \tag{9}$$

The absorber-tube average temperature (^{o}C) can be calculated as [20]:

$$T_{rt} = T_{g,m} + \frac{\dot{m} c_p \, Q_{usf} \left(T_{g,o} - T_{g,i} \right)}{h_{c,i} \, \pi \, D_{rt,o} \, L_{rt}} \tag{10}$$

The mean temperature of glycerin (^{o}C) can be expressed as:

$$T_{g,m} = \frac{T_{g,o} + T_{g,i}}{2} \tag{11}$$

The glycerin outlet temperature of absorber-tube (^{o}C) is expressed as:

$$T_{g,o} = T_{g,i} + \frac{Q_{usf}}{\dot{m} \, c_p} \tag{12}$$

The glycerin's heat transfer coefficient inside absorber-tube can be calculated as [32]:

$$h_{c,i} = \frac{K_g}{D_{rt,i}} \left[3.6 + \frac{0.0668 \left(\frac{D_{rt,i}}{L} \right) Re_g \, Pr_g}{1 + 0.04 \left[\left(\frac{D_{rt,i}}{L} \right) Re_g \, Pr_g \right]^{2/3}} \right] \tag{13}$$

Open Access
No. 38, March 2023, pp. 74-96

P- ISSN: 2220-5381
E- ISSN: 2710-1096

Reynolds number Re_g for this case is expressed as:

$$Re_g = \frac{4\,\dot{m}}{\pi\,\rho_g V_g\, D_{rt,i}} \tag{14}$$

The efficiency factor of the collector is expressed as:

$$F' = \frac{{}^{1}/_{U_L}}{\frac{1}{U_L} + \frac{D_{rt,o}}{h_{c,i} D_{rt,i}} + \frac{D_{rt,o}\ \ln\left({}^{D_{rt,o}}/_{D_{rt,i}}\right)}{2\,k_{rt}}} \tag{15}$$

The factor of heat removal can be determined as:

$$F_R = \frac{\dot{m}\,c_p}{A_{rto} U_L}\left[1 - \exp\left(-\frac{A_{rt,i}\ U_L\, F'}{\dot{m}\,c_p}\right)\right] \tag{16}$$

The hot storage tank new temperature after one hour is determined as:

$$T_{sh,new} = T_{sh,old} + \frac{\Delta t_{sh}}{m_{sh} C_p}\left[Q_{usf} - Q_{l1} - (UA_{sh})\left(T_{sh,old} - T_{amb}\right)\right] \tag{17}$$

The cold storage tank new temperature after one hour is determined as:

$$T_{sc,new} = T_{sc,old} - \frac{\Delta t_{sc}}{m_{sc}\, C_p}\left[Q_{acum} - Q_{l,ngh} + (UA_{sc})\left(T_{sc,old} - T_{amb}\right)\right] \tag{18}$$

$$Q_{acum} = Q_{l2} - Q_{l1} \tag{19}$$

3.2. Thermal Cooling System Absorbance Mathematical Modeling

The generator's energy and mass balances can be represented as:

$$Q_g = \dot{m}_{1,w} h_{1,w} + \dot{m}_{8,ss} h_{8,ss} - \dot{m}_{7,ws} h_{7.ws} \tag{20}$$

$$\dot{m}_{7,ws} = \dot{m}_{1,w} + \dot{m}_{8,ss} \tag{21}$$

The lithium bromide recycling rate equation for the mass equilibrium is calculated as following [6]:

$$\dot{m}_{7,ws}\, X_{7,ws} = \dot{m}_{8,ss}\, X_{8,ss} \tag{22}$$

where,

$$\dot{m}_{1,w} = \dot{m}_{2,w} = \dot{m}_{3,w} = \dot{m}_{4,w} \tag{23}$$

$$\dot{m}_{5,ws} = \dot{m}_{6,ws} = \dot{m}_{7,ws} \tag{24}$$

$$\dot{m}_{8,ss} = \dot{m}_{9,ss} = \dot{m}_{10,ss} \tag{25}$$

$$X_{1,w} = X_{2,w} = X_{3,w} = X_{4,w} = 0 \tag{26}$$

$$X_{5,ws} = X_{6,ws} = X_{7,ws} = X_{ws} \tag{27}$$

$$X_{8,ss} = X_{9,ss} = X_{10,ss} = X_{ss} \tag{28}$$

By substituting equations (21) and (22), we get on the mass flow equations for the strong and weak solution [2]:

$$\dot{m}_{8,\mathrm{ss}} = \frac{X_{7,ws}}{X_{8,ss} - X_{7,ws}}\,\dot{m}_{1,w} \tag{29}$$

$$\dot{m}_{5,ws} = \frac{X_{10,ss}}{X_{10,ss} - X_{5,ws}}\,\dot{m}_{4,w} \tag{30}$$

The condenser's energy balance can be represented as [5]:

$$Q_c = \dot{m}_{1,w}\left(h_{1,w} - h_{2,w}\right) \tag{31}$$

The expansion valve's energy balance can be represented as:

$$h_{2,\mathrm{w}} = \mathrm{h}_{3,\mathrm{w}} \tag{32}$$

$$h_{9,\mathrm{ss}} = \mathrm{h}_{10,\mathrm{ss}} \tag{33}$$

The evaporator's energy balance can be expressed as [5]:

$$Q_{\mathrm{e}} = \dot{m}_{4,\mathrm{w}}\,\mathrm{h}_{4,\mathrm{w}} - \dot{m}_{3,\mathrm{w}}\,\mathrm{h}_{3,\mathrm{w}} \tag{34}$$

So the cooling water mass flow rate equation can be calculated from the energy balance equation of the evaporator as follows [5]:

$$\dot{m}_{1,\mathrm{w}} = \frac{\mathrm{Q_e}}{(\mathrm{h}_{4,\mathrm{w}} - \mathrm{h}_{3,\mathrm{w}})} \tag{35}$$

The solution pump equation is expressed as:

$$w_p = \dot{m}_{6,\mathrm{ws}}\,\mathrm{h}_{6,\mathrm{ws}} - \dot{m}_{5,\mathrm{ws}}\,\mathrm{h}_{5,\mathrm{ws}} \tag{36}$$

Since the power of the mechanical pump is very low when compared to the generator power, then it will be neglected:

$$\mathrm{h}_{6,\mathrm{ws}} = \mathrm{h}_{5,\mathrm{ws}} \tag{37}$$

The absorber's energy balance can be written as:

$$Q_{abs} = \dot{m}_{4,\mathrm{w}} h_{4,w} + \dot{m}_{10,ss} h_{10,ss} - \dot{m}_{5,ws} h_{5.ws} \tag{38}$$

where, ($\mathrm{h}_{9,\mathrm{ss}} = \mathrm{h}_{10,\mathrm{ss}}$)

The overall energy balance is calculated using the following formula [6]:

$$Q_g + Q_e = Q_c + Q_{abs} \tag{39}$$

The heat exchanger's heat balance is expressed as:

Open Access
No. 38, March 2023, pp. 74-96

P- ISSN: 2220-5381
E- ISSN: 2710-1096

$$\dot{m}_{8,ss}\left(\mathrm{h}_{8,ss} - \mathrm{h}_{9,ss}\right) = \dot{m}_{7,ws}\left(\mathrm{h}_{7,ws} - \mathrm{h}_{6,ws}\right) \quad (40)$$

The heat exchanger's effectiveness can be computed as:

$$E_{\mathrm{hx}} = \frac{\mathrm{T_g} - \mathrm{T_8}}{\mathrm{T_g} - \mathrm{T_5}} \quad (41)$$

$$T_{\mathrm{abs}} = \mathrm{T_6} = \mathrm{T_5} \quad (42)$$

From the heat exchanger's effectiveness equation (41), we extract (T_9), which are:

$$T_9 = T_g - E_{hx}\left(T_g - T_{abs}\right) \quad (43)$$

And from the heat exchanger equilibrium equation (40), we extract ($h_{7,ws}$), which are:

$$h_{7,ws} = \frac{\dot{m}_{8,ss}}{\dot{m}_{7,ws}}\left(h_{8,ss} - h_{9,ss}\right) + h_{6,ws} \quad (44)$$

The absorption system's performance coefficient (cop) is calculated as [6]:

$$cop = \frac{Q_e}{Q_g} = \frac{\dot{m}_{1,\mathrm{w}}\left(\mathrm{h}_{4,\mathrm{w}} - \mathrm{h}_{3,\mathrm{w}}\right)}{\dot{m}_{1,w}h_{1,w} + \dot{m}_{8,ss}h_{8,ss} - \dot{m}_{7,ws}h_{7.ws}} \quad (45)$$

The input data required to simulate the overall processes are absorption cycle capacity, hourly ambient temperature, hourly wind velocity, hourly solar radiation intensity, generator, condenser, evaporator, absorber temperatures range and heat exchanger effectiveness. The list of nomenclatures for variable symbols used in the modeling of mathematical calculations is shown in Table (1).

Table (1) List of nomenclatures.

Symbol	Meaning	Units
$\boldsymbol{\eta}$	Efficiency of solar thermal concentrated collector	---
Q_{usf}, Q_{l1}, Q_{l2}, $Q_{l,ngh}$, Q_{acum}	Useful heat, building required cooling, produced cooling, night building and accumulated loads respectively	W
I_b	Collector solar intensity	W/m^2
A_{ape}	Aperture area of the reflector	m^2
F_R	Heat removal factor	---
F'	Efficiency factor of the collector	---
H_{ab}	Absorbed solar energy	W/m^2
A_{rto}	Receiver tube outside area	m^2
$T_{g,i}$, $T_{g,o}$, $T_{g,m}$	Inlet, outlet and mean temperatures of glycerin respectively	ºC
T_{amp}	Ambient temperature	ºC
w , L	Collector width and length respectively	m

Open Access
No. 38, March 2023, pp. 74-96

P- ISSN: 2220-5381
E- ISSN: 2710-1096

$D_{rt,i}$, $D_{rt,o}$, L_{rt}	Inside diameter, outside diameter and length of receiver (absorber) tube respectively	m
$\tau, \alpha, \rho, \gamma$	The transmittance, the absorbance, the reflectiveness and the objection coefficient (0.99 in this study) of the absorber tube respectively	---
θ	Angle of the collector	°
U_L	Overall coefficient of the heat loss	W/m^2.°C
h_{win}	Wind speed heat transfer coefficient	W/m^2.°C
V	Wind velocity of free stream	m/s
$h_{ra,rt-sky}$	Heat transfer coefficient by radiation between the absorber tube and its surroundings	W/m^2.°C
σ	Stefan Boltzmann constant (5.6697×10^8)	---
ε_{rt}	Absorber-tube emissivity	---
T_{sky}	Temperature of sky	°C
T_{rt}	Absorber-tube average temperature	°C
$\dot{m}$	Flow rate of glycerin	kg/sec
cp	Glycerin's specific heat at constant pressure	J/kg.°C
$h_{c,i}$	Glycerin's heat transfer coefficient inside absorber-tube	W/m^2.°C
K_g , k_{rt}	Thermal conductivities of glycerine and absorber-tube	W/m.°C
ρ_g	Density of glycerin	kg/m^3
V_g	Velocity of glycerin	m/sec
Pr_g , Re_g	Prandtl-number, Reynolds number of glycerin	---
$T_{sh,new}$, $T_{sh,old}$	New and old temperatures of hot storage tanks	°C
$T_{sc,new}$, $T_{sc,old}$	New and old temperatures of cold storage tanks	°C
Δt_{sh}, Δt_{sc}	Time differences between an hour and an hour for hot and cold storage tanks	sec
m_{sh} , m_{sc}	Mass flow rates of hot and cold storage tanks	kg/sec
UA_{sh} , UA_{sc}	Hot and cold storage tanks thermal losses coefficients	(W/°C)
Q_g, Q_c, Q_e, Q_{abs}	Generator, condenser, evaporator and absorber energies respectively	W
w_p	Pump of solution	W
$\dot{m}_{1,w}$	Mass flow rate of water refrigerant	kg/sec
$\dot{m}_{7,ws}$	Mass flow rate of weak solution	kg/sec
$\dot{m}_{8,ss}$	Mass flow rate of strong solution	kg/sec
$h_{1,w}$, $h_{2,w}$, $h_{3,w}$, $h_{4,w}$	Saturated water vapour at a high temperature, saturated water liquid, saturated water liquid and saturated water vapour enthalpies respectively	kJ/kg
$h_{5,ws}$, $h_{6,ws}$, $h_{7,ws}$	Enthalpy of weak solution	kJ/kg
$h_{8,ss}$, $h_{9,ss}$, $h_{10,ss}$	Enthalpy of strong solution	kJ/kg

Open Access
No. 38, March 2023, pp. 74-96

P- ISSN: 2220-5381
E- ISSN: 2710-1096

X	Concentration percent of lithium bromide	---
$X_{7,ws}$, $X_{8,ss}$	Concentration percent of lithium bromide in the weak and strong solutions	---
E_{hx}	heat exchanger's effectiveness	---
T_g , T_c, T_e, T_{abs}	Generator, condenser, evaporator, and absorber temperatures respectively	ºC
T_5	The temperature of the weak solution when entering the pump	ºC
T_8 , T_9	The temperatures of the strong solution at the heat exchanger inlet and exit	ºC
cop	Absorption system's performance coefficient	---

4. Results and Discussion

Figure (3) shows the change of the temperature of the hot tank of glycerin capacity of (0.55 m^3) in 20th May with the change of the area of the solar collector with a load and without load within (24) hours. The area of the solar collector is increased several times to reach an area of (11.8 m^2) by proving the capacity of the hot tank to raise its temperature to reach the highest temperature (184°C) in the presence of load (SHL). The condition of the load in the same area and the capacity of the previous tank rise the temperature of the hot tank to a degree (198.88°C) (SHNL) and therefore shows the importance of the presence of the load in its effect on the temperature of the hot tank. Figure (4) shows the temperature change of the cold tank of the glycerin capacity (1.5 m3) for the day (20 May) with a load (SCL) and no load (SCNL) within (24) hours, select the cold tank with a capacity (1.5 m^3) to be charged with excess energy during the work of the absorption system and note that a constant temperature remains unchanged until the cold tank starts charging with excess capacity and its temperature drops to (1.03℃) at 11 pm then the temperature of the cold tank to rise (1.3℃) due to the thermal losses of the tank inside the room and the interruption of charging it to stop the absorption system to work and in the case of a load it is noted that the temperature of the cold tank to a degree (2.5℃) due to processing space adapted by the cold-powered tank needed to adapt.

Figure (5) shows the change of temperature of the hot tank of the glycerin capacity (1.255 m^3) for the day (20 May) with the change of the area of the solar collector with a load and without a load within (24) hours. The area of the solar collector was increased to (13.44 m^2) to raise the temperature of the hot tank with a capacity (1.255 m^3) up to a limit of (137.1℃) with a load and it was observed that the tank temperature after midday is greater than the temperature of the hot tank with a capacity (0.53 m^3) after midday of the same day. In the absence of a load, the

Open Access
No. 38, March 2023, pp. 74-96

P- ISSN: 2220-5381
E- ISSN: 2710-1096

temperature of the hot tank reaches (149.31℃) for the day (20 May) due to the increased heat energy stored.

Figure (6) shows the temperature change of the hot tank of the glycerin capacity (1.3 m^3) for the day (20 May) with the change of the area of the solar collector concentrates in the presence of a load and without a load within (24) hours. Several areas of concentrated solar collector were used up to an area of (16.32 m2) to reach the highest temperature of the hot tank (167.4℃) in the presence of a load. In the absence of a load, the temperature of the hot tank up to a degree (179.59 ℃). Figure (7) shows the change in the temperature of the glycerin hot tank with a capacity of (0.55 m^3) for the day (June 8) with the change in the area of the central solar collector, with and without load, within (24) hours. The area of the concentrated solar collector is increased several times to reach an area of (12.48 m^2) as the capacity of the hot tank is fixed to raise its temperature to reach the highest temperature (193.52℃) in the presence of a load. In the case of no-load and with the same space and capacity of the previous tank, the temperature of the hot tank is raised to 208.6℃. The decrease in the tank temperature is observed after midday due to thermal losses as well as sunset. Figure (8) shows the change in the temperature of the cold tank of glycerin with a capacity of (1.5m^3) for the day (June 8) with and without load within (24) hours. We note that the temperature remains unchanged until the cold tank begins to be charged with surplus energy, so its temperature drops to (0.57℃) at 11 pm. Then it is noted that the temperature of the cold tank rises to (0.9℃) due to the thermal losses of the tank inside the room and the interruption of charging for it to stop the sorption system from working. In the event of a load, the temperature of the cold tank is noted to rise to a degree (1.99) due to the supply of the air-conditioned space by the cold tank with the energy needed for adaptation. Figure (9) shows the change in the temperature of the glycerin hot tank with a capacity of (1.39 m^3) for the day (June 8), with the change in the area of the central solar collector with and without load within (24) hours. The area of the concentrated solar collector was increased to (13.63 m^2) to raise the temperature of the hot tank to (120.48℃) in the presence of a load. In the absence of a load, the temperature of the hot tank reaches (132.37℃). Figure (10) shows the change in the temperature of the cold storage tank of glycerin with a capacity of (1.6 m^3) for the day (June 8) with and without pregnancy during (24) hours. We note that the temperature remains unchanged until the cold tank starts charging with surplus energy, so its temperature drops to (1.4℃) at (11) in the evening. Then it is noted that the temperature of the cold tank rises to (1.89) ℃ due to the

Open Access
No. 38, March 2023, pp. 74-96

P- ISSN: 2220-5381
E- ISSN: 2710-1096

thermal losses of the tank inside the room and the interruption of charging for it to stop the sorption system from working. In the event of a load, the temperature of the cold tank is noted to rise to a degree (3.3℃) due to the reason mentioned in the previous section. Figure (11) shows the working hours of the glycerin hot tank with a capacity of (1.4 m^3) for the day (June 8th), with an area of a concentrated solar collector (16.7 m2) to equip the sorption system with a temperature of no less than (65℃). After the temperature of the hot tank rose at sunrise, it was found that the temperature of the tank reached (69.27℃) at 9 am, as it started preparing the sorption system until 12 pm. That is, the number of working hours amounted to (15) hours, and this The increase in the number of working hours under the same conditions and loads as the previous tanks due to the increase in stored heat energy. The intensity of the solar can be illustrated for (20/May and 8/June) as in Figure (12). The change in the load values of the air-conditioned space is gradually at sunrise and reaches the highest value shortly after midday, then decreases to the lowest values at sunset for each of the two specified days. This indicates the effect of the intensity of direct solar radiation mainly on the load values of the air-conditioned space. The coefficient of performance for generator (Tg), condenser (Tc), evaporator (Te), and absorber (Tabs) temperatures are shown in Figure (13).

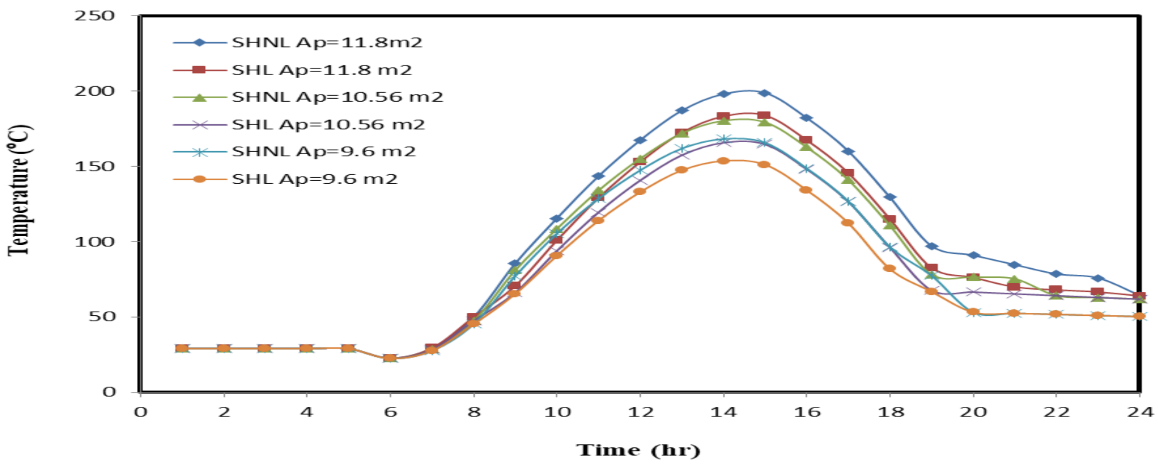

Fig. (3): Changing the temperature of the hot tank of glycerin with the working hours of the tank with a capacity of (0.55 m^3) at (20 May) and in different areas of the solar collector.

Open Access
No. 38, March 2023, pp. 74-96

P- ISSN: 2220-5381
E- ISSN: 2710-1096

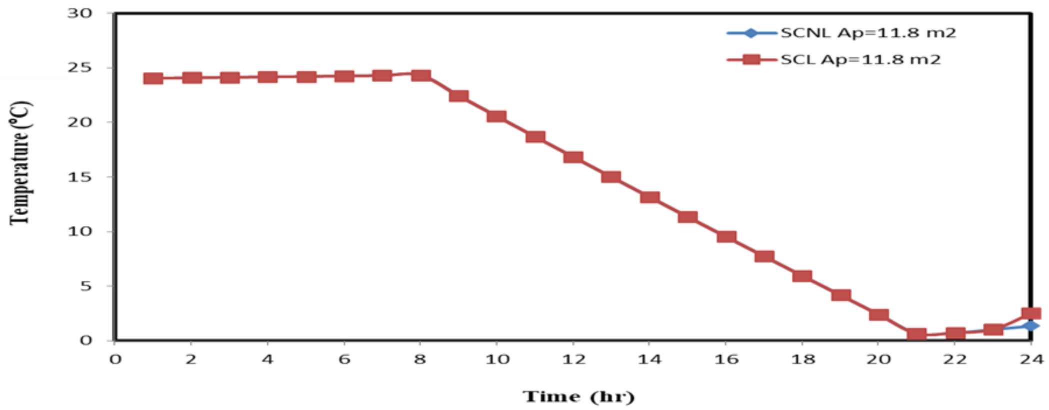

Fig. (4): The temperature changes of the cold tank of the glycerin with the working hours of a tank with a capacity (1.5 m3) on the day (20 May).

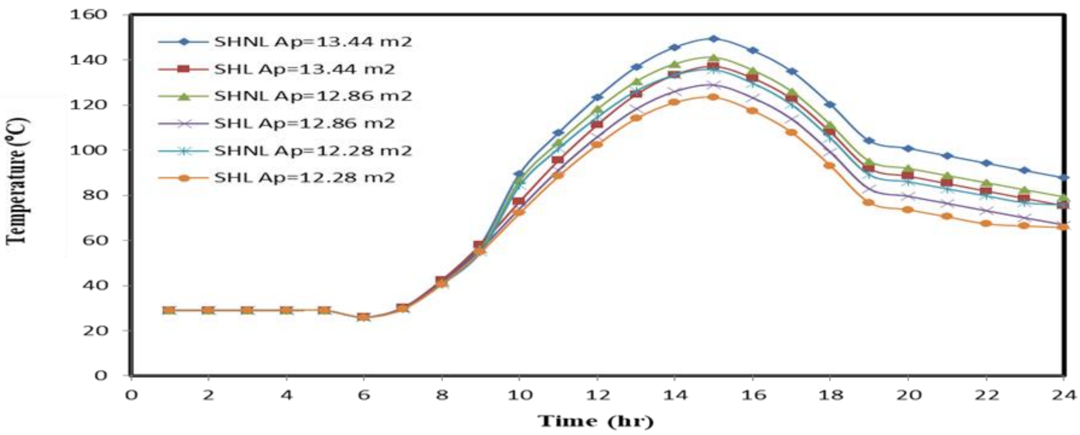

Fig. (5): The temperature of the hot tank of the glycerin was changed with the working hours of the tank with a capacity of (1.255 m3) on (20 May) and in different areas of the solar collector.

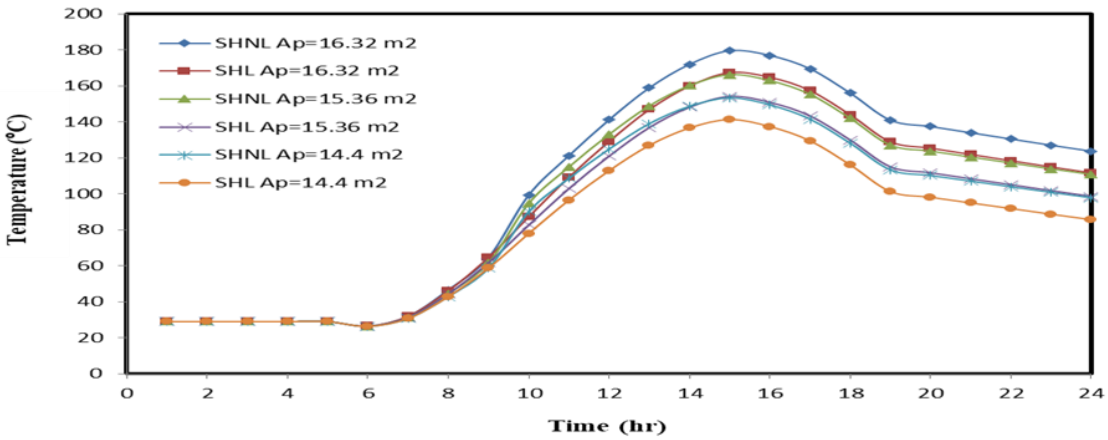

Fig. (6): The temperature of the hot tank of the glycerin changed with the working hours of the tank with a capacity (1.3 m3) at (20 May) and in different areas of the solar collector.

Open Access
No. 38, March 2023, pp. 74-96

P- ISSN: 2220-5381
E- ISSN: 2710-1096

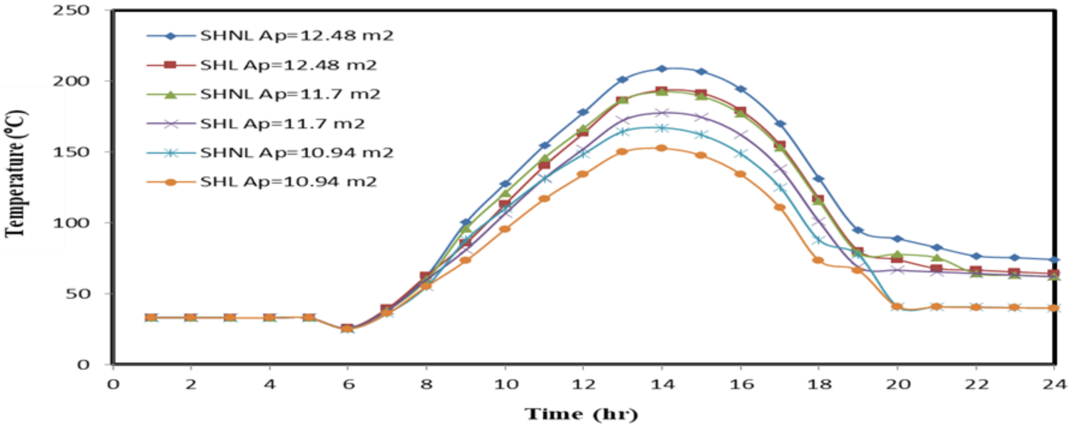

Fig. (7): Changing the temperature of the hot tank of the glycerin with the working hours at a tank with a capacity (0.55 m3) for the day (8 June) and in different areas of the solar collector.

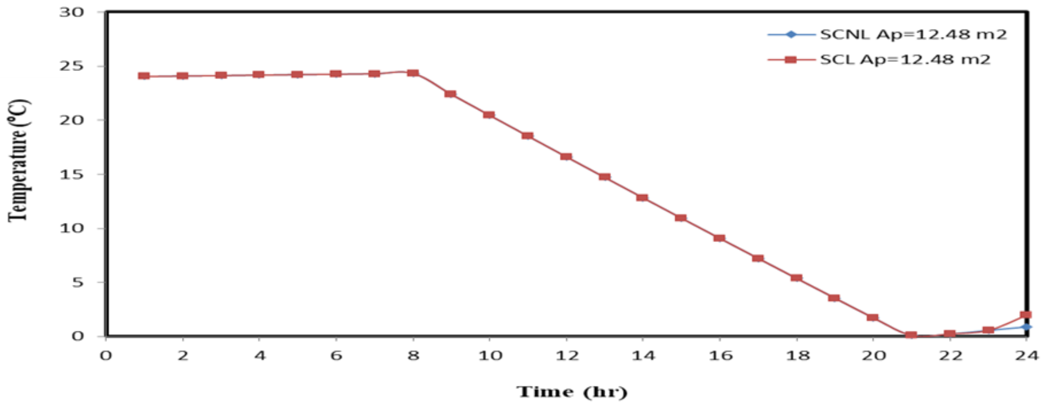

Fig. (8): Temperature with the working hours of the cold tank of glycerin with a capacity (1.5 m3) and for the day (8 June).

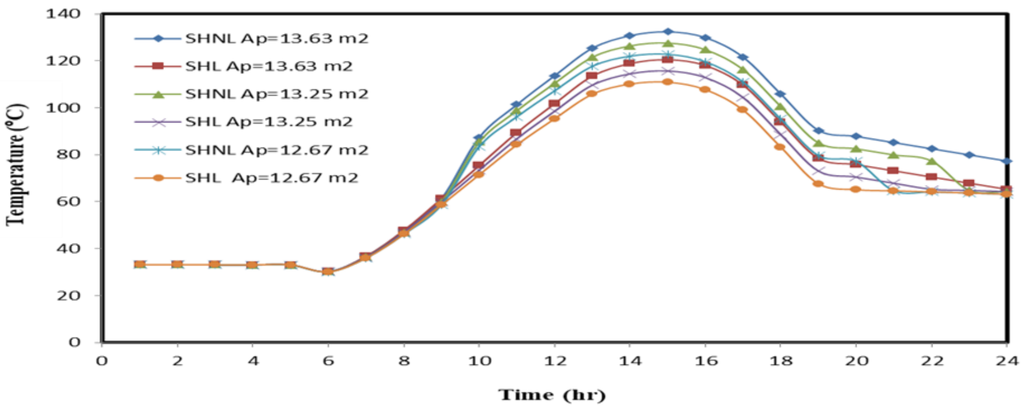

Fig. (9): Changing the temperature of the hot tank of the glycerin with the working hours at a tank with a capacity (1.39 m3) for the day (8 June) and in different areas of the solar collector.

Journal of Petroleum Research and Studies

Open Access
No. 38, March 2023, pp. 74-96

P- ISSN: 2220-5381
E- ISSN: 2710-1096

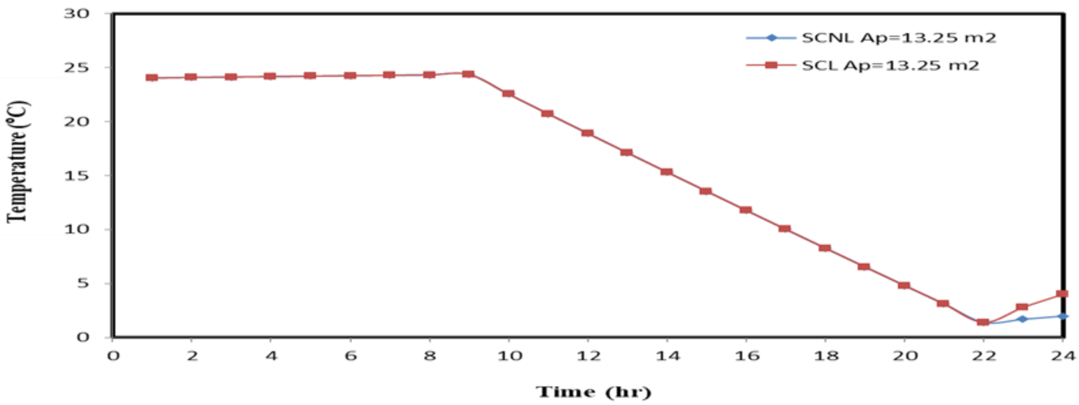

Fig. (10): Temperature with the working hours of the cold tank of the glycerin with a capacity (1.6m3) and for the day (8 June).

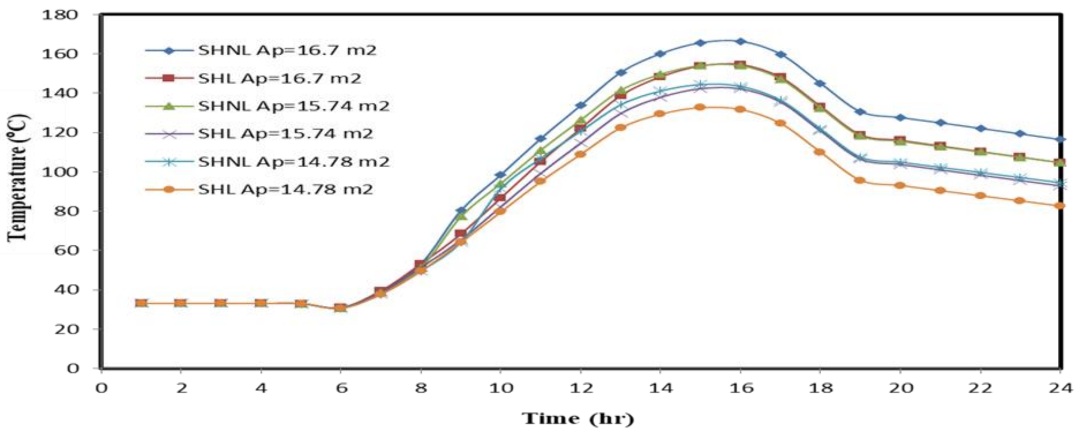

Fig. (11): Changing the temperature of the hot tank of the glycerin with the working hours at a tank with a capacity (1.4 m3) for the day (8 June) and in different areas of the solar collector.

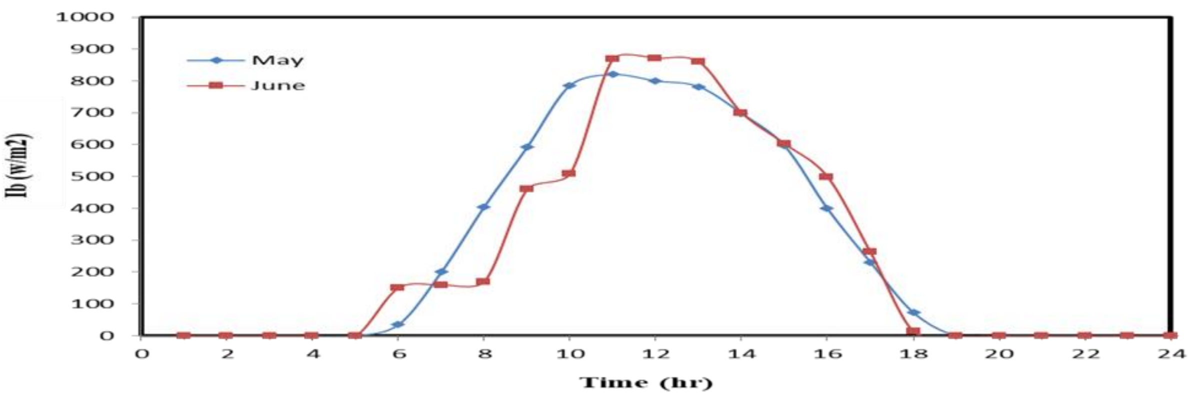

Fig. (12): Intensity of the son for 20/May and 8/June.

Journal of Petroleum Research and Studies

Open Access
No. 38, March 2023, pp. 74-96

P- ISSN: 2220-5381
E- ISSN: 2710-1096

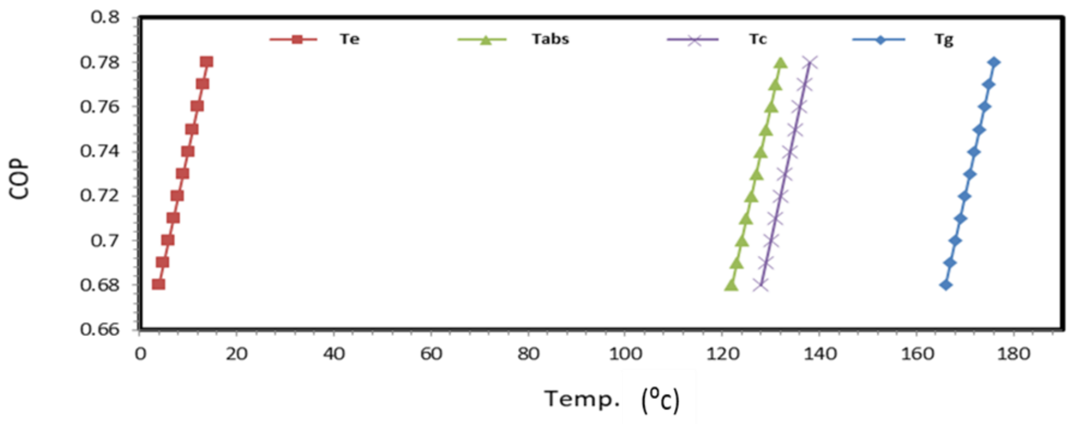

Fig. (13): Coefficient of performance of absorber, generator, condenser and evaporator with the temperature variation.

5. Conclusions

Investigation was conducted to study the effect of changing the thermal storage capacities of hot and cold storage tanks and the solar collector area on the performance of the absorption air conditioning cycle. The water-lithium bromide solution was used as a fluid in the sorption cycle, and glycerin was used in the hot and cold tank cycle. According to the results of the research obtained, the following points were concluded:

1. The best and most suitable size for the hot tank is (0.55 m3), and for the cold tank (1.5 m3), and the best suitable area for the central solar collector is (11.7 m2), which can provide longer operating hours.

2. To achieve high temperatures, the amount of usable energy is directly controlled by the concentric area of the solar collector, and the volume of the heated tank is directly related to the area of the solar collector.

3. Determination of the best capacity of the hot tank, the size of the cold tank is increased by increasing the amount of energy collected by the solar collector, and this depends on the presence of the cold tank and the number of hours.

4. Increasing in the intensity of solar radiation, the size of the cold tank and the cooling loads that must be carried out in space increase.

5. Ultimately the higher the temperature of the generator, the higher the system's coefficient of performance (COP). The lowest COP value (0.68) is used to ensure that the system runs for longer periods of time.

Open Access
No. 38, March 2023, pp. 74-96

P- ISSN: 2220-5381
E- ISSN: 2710-1096

References

[1] R.Foster,M.Ghassemi,A.Cota,"Solar energy :Renewable Energy and the Environment", USA,CRC press ,2010.

[2] Hashim A.Hussain, "Development of Absorption Cooling System Work by Using Solar Energy". Al-Rafidain Journal for Sciences, 32, pp131-160, 2013.

[3] Abdulmunem R. Abdulmunem, Abdullateef A. Jadallah , Hisham A. Hoshi, Mohammed H. Jabal," Effect of Colored Filters on PV Panels Temperature and Performance under Baghdad Meteorological Condition" Tikrit Journal of Engineering Sciences, 25 (4) ,pp46 – 50, 2018.

[4] W. Weiss, M. Rommel," Process heat collectors ", Austria, AEE, INTC, Glesidorf, Feldgasse19 (33), pp1-58, 2008

[5] I. Dincer, "Refrigeration System and Applications ", England, WILEY, 2003.

[6] Khalid Ahmed Al-Joudi. "Principles of Air Conditioning and Crystallization Engineering". Basra: University of Basra, 1986.

[7] Mittal.V, Kasana. K.S. and Thakur N.S.," Performance evaluation of solar absorption cooling system of Bahal (Haryana)", J. Indian Inst.Sci, 85, pp295-305, 2005.

[8] Philippe.J, Morau.D, Lucas.F, Garde .F, Boyer .H," Simulation of a solar absorption cooling system",France,university Laboratoire de Reunion,117,pp1-8,2007.

[9] Salagado. R, Rodriguez .P, Lecuona. A, Rodriguez. M.C," Optimized design of hot water storage in solar thermal cooling Facilities",Spain, ,University Carlos III de Madrid ,ITEA Research croup,1-8,2008.

[10] V Mittal,K S Kasana NS Thakur. The study of solar absorption air-conditioning systems. Journal of Energy in Southern Africa, 16(4), pp59-67, 2005

[11] Vidal. H, Escobar. R, Colle. S, "Simulation and optimization of a solar driven air conditioning system for a house in Chile", Chile, ISES Solar world congress, 42, pp844-853, 2009.

[12] Ming. Q, Hongxi. Y, Archer. D," A solar thermal cooling and heating system for a building: Experimental and model based performance analysis and design", Solar energy, 84, pp166-182, 2010.

[13] Govindaraj, Rahulram, Ramalingom," Performance studies of a solar parabolic trough collector with a thermal energy storage system",India,Energy, 47, pp395-402, 2012 .

Open Access
No. 38, March 2023, pp. 74-96

P- ISSN: 2220-5381
E- ISSN: 2710-1096

[14] Pietruschka. D, Jakob.U, Hanby.V, Eicker.U, “Simulation Based optimization and experimental investigation of a solar cooling and heating system ", Spain, Proceedings of Second international conference solar air conditioning, 24, pp1-6, 2007.

[15] Pongtornkulpaanich. A, Thepa.S, Amornkibamrung.M, Butcher.C, “Experience with fully operational solar –driven 10-ton LiBr/H2O single-effect absorption cooling system in Thailand ", University of Technology, Elsevier, 22, pp943-949, 2007.

[16] Pietruschka.D, Jakob.U, Hanby.V, Eicker.U," Simulation Based Optimization of a Newly Developed System Controller for Solar Cooling and Heating Systems ", Germany, Eurosun Proceedings of the Conference Eurosun, pp1-8, 2008.

[17] Ortiz.M, Mammoli.A, Vorobieff.P," A TRNSYS Model of a solar Thermal system with Thermal storage and absorption cooling”, Mexico, ASEE American Society for Engineering Education, University new Mexico,12,pp1-13, 2008 .

[18] Ortiz.M, Barsun.H, He.H, Peter.V, Andrea.A," Modeling of a solar-assisted HVAC system with thermal storage ", USA, University of New Mexico, Energy and Buildings, 42, pp500-509, 2010.

[19] Agyenim.F, Knight.I, Rhodes.M," Design and experimental testing of the performance of an outdoor LiBr/H2O solar thermal absorption cooling system with a cold store ", University of Caridff, Solar energy, 84, pp735-744, 2010.

[20] Hang.Y, ming.Q," The impact of hot and cold storages on a solar absorption cooling system for an office building ", International high performance buildings conference, USA, 3472, pp1-8, 2010.

[21] Marc.O, sinama.F, Lucas.F," Decision making tool to design solar cooling system coupled with building under tropical climate”, France, Energy and buildings, 49, 28-36, 2012.

[22] Faiza Mahdi Hadi. Simulation Study and Comparison Green Freeze Technology Utilizing with Theory of Different Adsorption Working Pairs of Solar Adsorption Refrigeration. Journal of Engineering and technology, 30(3), pp84-97, 2012.

[23] Al-Sammarraie ATA, Mahdi MS “Theoretical Study of Heat Transfer through a Sun Space Filled with a Porous Medium”,Tikrit Journal of Engineering Sciences;23(2),pp10-20, 2016.

Open Access
No. 38, March 2023, pp. 74-96

P- ISSN: 2220-5381
E- ISSN: 2710-1096

[24] Jassim AH, Rahman MM, Hamada KI, Ishak M, Tahseen TA. “Hybrid CFD-ANN scheme for air flow and heat transfer across in-line flat tubes array” Tikrit Journal of Engineering Sciences; 25 (2), pp59-67, 2018.

[25] Hamdoon OM, Al-Ali BM, “Modeling and Simulation of a Desiccant Evaporative Cooling System” Tikrit Journal of Engineering Sciences, 26(3), pp10- 18, 2019.

[26] M. H. Zaidan, H. J. Khalaf, and B. A. Ahmed, “Thermal analysis of a solar absorption cooling system with hot and cold storage tanks,” J. Adv. Res. Fluid Mech. Therm. Sci., vol. 50, no. 1, pp. 67–80, 2018.

[27] G. Singh and R. Das, “Energy saving assessment of triple-hybrid vapor absorption building cooling system under hot-dry climate,” *Am. Soc. Mech. Eng. Power Div. POWER*, vol. 2021-July, 2021.

[28] A. Al-Falahi, F. Alobaid, and B. Epple, “Design and thermo-economic comparisons of large scale solar absorption air conditioning cycles,” Case Stud. Therm. Eng., vol. 22, 2020.

[29] Darkwa.j, Fraser.S, Chow.D, “Theoretical and practical analysis of an Integrated solar hot water-powerd absorption cooling system ", Energy, 31, pp296-309, 2011.

[30] Ismael.M, Salman.M, Adnan.G, “Analysis of solar powered air conditioning systems for residential applications", Thi-Qar university journal for engineering sciences, 3, pp15-27, 2012.

[31] Yaghoubi M, Ahmadi F, Bandehee M. Analysis of Heat Losses of Absorber Tubes of Parabolic Trough Collector of Shiraz (Iran) Solar Power Plant. Journal of Clean Energy Technologies; 1 (1):33-37, 2013.

[32] Holman.J. P, "Heat Transfer", McGraw-Hill, Tenth Edition, pp283, 2010.